Identification of a Highly Functional Effector CD8$^+$ T Cell Program after Transplantation in Mice and Humans

Gregory S. Cohen[1], Joel S. Freibaum,[1] Riley P. Leathem,[1] Ryo Hatano,[2] Chikao Morimoto,[2] Scott M. Krummey[1]*

[1]Department of Pathology, Johns Hopkins School of Medicine, Baltimore, MD, 21205, USA

[2]Department of Therapy Development and Innovation for Immune Disorders and Cancers, Graduate School of Medicine, Juntendo University, Tokyo 113-8421, Japan

*Correspondence: skrumme1@jhmi.edu

Keywords: effector CD8$^+$ T cells, alloimmunity, costimulation blockade

ABSTRACT

Acute T cell mediated rejection of allografts remains a significant risk factor for early graft loss. Our prior work defined a population of graft-specific $CD8^+$ T cells positive for the activated receptor CD43 (expressing the 1B11 epitope) that form during acute rejection, leading us to further understand the in vivo fate and clinical relevance of this population. We found that during acute rejection, the $CD43^+ICOS^+$ phenotype was sensitive for proliferative graft-specific $CD8^+$ T cells. We evaluated whether CD43 1B11 signaling could impact graft survival, and found that CD43 1B11 mAb treatment could overcome costimulation-blockade induced tolerance in the majority of mice. Using an adoptive transfer approach, we investigated the fate of CD43 $1B11^+$ and CD43 $1B11^-$ $CD8^+$ T cell populations, and found that CD43 $1B11^+$ $CD8^+$ T cells were more persistent three weeks after transplantation. A portion of CD43 $1B11^-$ $CD8^+$ T cells converted to CD43 $1B11^+$, while CD43 $1B11^+$ $CD8^+$ T cells retained CD43 $1B11^+$ status. In healthy human donors, we found that the CD43 1D4 clone, which identifies the large CD43 isoform, defines a population of antigen-experienced $CD8^+$ T cells independent of the canonical $CD8^+$ T cell populations. CD43 $1D4^+$ $CD8^+$ T cells were efficient cytokine-producers after stimulation. In scRNA-seq analysis of graft-infiltrating cells from renal transplant patients experiencing acute rejection, a population of SPN^+GCNT1^+ $CD8^+$ T cells had an effector phenotype that includes high expression of IFNG, ICOS, and perforins/granzymes. Together, these data provide evidence that the CD43 1B11 expression defines a proliferative and persistent population of $CD8^+$ T cells in mice, and that an analogous population of antigen-experienced $CD8^+$ T cells that participate in allograft rejection.

INTRODUCTION

Despite technical advances that have vastly improved early outcomes after solid organ transplant, the long-term survival of transplanted organs has remained stagnant for over three decades.[1,2] A major source of graft loss is immune-mediated rejection, which was traditionally classified as acute or chronic based on its occurrence early or late after transplantation.[3,4] While chronic rejection was assumed to be the major contributor to graft failure that occurs many years after transplant, recent studies have shown that the cumulative impact of T cell mediated acute rejection is a major risk factor for later graft loss.[5–7] Thus, the development of original approaches that specifically prohibit and/or treat T cell-mediated cellular rejection are highly important in order to improving outcomes post-transplant. While both $CD4^+$ and $CD8^+$ T cells participate in acute rejection, multiple studies have highlighted that $CD8^+$ T cells, which have potent cytolytic and cytokine-producing functions, mediate rejection in pre-clinical models and patients.[8–12]

$CD8^+$ T cells populations are heterogeneous and shaped by the priming environment, including antigen levels, antigen affinity, inflammation, and cosignaling.[13–18] During an acute immune response, activated $CD8^+$ T cells are broadly divided into short-lived effector cell (SLEC) populations and longer-lived memory precursor populations. After viral and bacterial infection, the NK-cell receptor KLRG-1 is the canonical/best-defined marker for SLEC, although the function of this receptor is not clear.[19,20] In the context of chronic antigen exposure, stem-like precursor populations feed into terminally differentiated effector populations.[21–23] Each of these population dynamics have largely been defined outside the context of transplantation, which has unique mechanisms of antigen presentation and inflammation compared with infections and tumor immunity.

Our prior work established that, in contrast to protective immunity, very little KLRG-1 is expressed on graft-specific $CD8^+$ T cells during acute allograft rejection.[24] We found that, in contrast, graft-specific effectors acutely upregulated expression of the activated CD43 receptor

during graft rejection. CD43 is a transmembrane sialomucin which is broadly expressed on leukocytes, and has complex functions in cellular adhesion and trafficking, as well as cellular signalling.[25–28] However, T cell activation elicits the core-2 O-glycosylation of CD43 by the glycosyltransferase GCNT1,[29,30] which is denoted by the binding of the CD43 1B11 antibody clone. Our prior work showed that CD43 1B11 $CD8^+$ T cells were potent effectors that expressed highly levels of Granzyme B, the cytokines IFN-γ/TNF-α, and rapidly infiltrated allografts.[21]

In the current study, we further delineated the function of this population in mice and humans. We demonstrate that treatment of tolerant mice with the CD43 1B11 mAb *in vivo* elicits graft rejection, and that CD43 $1B11^+$ $CD8^+$ T cells are a persistent and terminal phenotype. In humans, we identified an analogous $CD8^+$ T cell population that are denoted by expression of the CD43 mAb clone 1D4. CD43 $1D4^+$ $CD8^+$ T cells had an antigen-experienced phenotype and were efficient producers of IFN-γ and TNF-α after stimulation. Finally, we investigated the graft-infiltrating $CD8^+$ T cells during acute rejection of kidney allografts, and found that a population of *SPN*$^+$*GCNT1*$^+$ that is defined by expression of markers of recent antigen-experience (*PDCD1, ICOS*) and effector molecules (granzymes, perforin, and IFN-γ). Together, these data provide new insight into the program of $CD8^+$ T cells that respond to allografts, and has translational implications for new approaches to prevent acute rejection.

RESULTS

The CD43$^+$ICOS$^+$ phenotype specifically identifies proliferative graft-specific CD8$^+$ T cells

Relative to protective immune responses, transplantation elicits relatively weak expansion of graft-specific CD8$^+$ T cells.[24,31] Our recent study showed that a population of CD43$^+$ICOS$^+$ cells forms among graft-specific CD8$^+$ T cells during acute rejection.[24] We wanted to evaluate whether CD43$^+$ICOS$^+$ phenotype can be used to identify the relatively rare proliferative CD8$^+$ T cells after transplantation. We evaluated graft-specific L^d QL9 tetramer$^+$ and total "bulk" CD8$^+$ T cells in H-2^b C57Bl/6 mice that received an H-2^d Balb/c skin graft on day 14 post-graft **(Figure 1A)**. We first measured the proliferative capacity of CD8$^+$ T cells using expression of Ki67, which denotes recently divided or actively proliferating T cells. The canonical activation markers CD44^{hi} or CD62L^{lo} were highly sensitive, but not specific for Ki67$^+$ cells **(Figure 1B)**, as all Ki67$^+$ CD8$^+$ T cells were found within these respective populations, but many CD44^{hi} and CD62L^{lo} cells were Ki67$^-$. We next evaluated the frequency of Ki67$^+$ cells among CD8+ T cells expressing the activation markers KLRG-1, CXCR3, CD43 1B11, and ICOS. As previously published, we found that very few KLRG-1$^+$ cells were elicited during acute rejection **(Figure 1B)**, precluding further meaningful analysis of KLRG-1$^+$Ki67$^+$ cells. We found that 66% and 43% of CXCR3$^+$ cells were Ki67$^+$ in the L^d QL9$^+$ and bulk CD8$^+$ T cell compartments, respectively **(Figure 1B)**. However, both CD43 1B11$^+$ and ICOS$^+$ populations were highly enriched for Ki67$^+$ CD8$^+$ T cells **(Figure 1B)**.

As Ki67 does not distinguish previously from actively proliferating cells, we directly visualized the proliferation of CD8$^+$ T cells during acute rejection using CellTrace Violet. We adoptively transferred polyclonal naïve CD45.1 CD8$^+$ T cells that were labeled with CellTrace Violet (CTV) proliferation dye into naïve C57Bl/6 (CD45.2) hosts, and transplanted Balb/c skin grafts the following day **(Figure 1C)**. After 14 days, we identified the graft-specific L^d QL9$^+$ CD8+ T cells and bulk CD8+ T cells using magnetic column enrichment. In parallel, we transferred

CTV Thy1.1$^+$ OT-I CD8$^+$ T cells into C57Bl/6 hosts and provided Act-mOVA skin grafts to compare the proliferative response **(Figure 1C)**. We evaluated the phenotype of the divided and undivided CD8$^+$ T cell populations. CD43$^+$ICOS$^+$ cells were not found within the undivided populations. A fraction of proliferated OT-I and bulk CD8$^+$ T cells were CD43$^+$ICOS$^+$ **(Figure 1C)**. However, nearly all of the L^d QL9$^+$ CD8$^+$ T cells were CD43$^+$ICOS$^+$ **(Figure 1C)**. These data demonstrate that CD43$^+$ICOS$^+$ phenotype can sensitively identify graft-specific CD8$^+$ T cells that have undergone cell division after transplantation.

CD43 mAb treatment overcomes tolerance to induce graft rejection.

The CD43 mAb clone 1B11 identifies the activated glycoform of CD43. The effect of this antibody on T cell function is unknown. We reasoned that because CD43 1B11$^+$ CD8$^+$ T cells are potent effectors, that signaling through this receptor would elicit graft rejection. Cross-linking of the 1B11 mAb *in vitro* resulted in a costimulatory signal (data not shown). To test the effect of the CD43 1B11 pathway on graft rejection in vivo, we induced tolerance via treatment with costimulation blockade (CTLA-4 Ig and CD40L mAb; **Figure 2A**), and treated mice with CD43 1B11 mAb on day 8-14, which corresponds to the initial expression of CD43 1B11 epitope on CD8$^+$ T cells.[24] We found that while costimulation blockade induced graft survival to 30 days, treatment with CD43 1B11 elicited graft rejection in 63% of mice by day 20 **(Figure 2B)**. We evaluated the phenotype of circulating CD8$^+$ T cells during this treatment regimen. While costimulation blockade elicited few activated effector CD8$^+$ T cells, mice treated with CD43 1B11 had a higher frequency of CD62L^{lo}CD27^{lo} T cell population **(Figure 2C)**. This population is highly proliferative, as denoted by expression of Ki67 **(Figure 2D)**. Together, these data demonstrate that activation of the CD43 1B11 signaling pathway is critical for acute rejection, and can overcome transplantation tolerance.

CD43 1B11 defines a persistent CD8$^+$ T effector population after transplantation

CD43$^+$ 1B11 CD8$^+$ T cells are not found in naïve CD8$^+$ T cells. After transplantation, the frequency of CD43 1B11$^+$ CD8$^+$ T cells peaks around 10-14 and begins to contract by day 21 post-graft. However, it is not clear whether CD43 1B11$^+$ CD8$^+$ T cells are persistent or rapidly contract after encounter with antigen. We used an adoptive transfer approach to test the relative survival and phenotypic conversion between CD43 1B11$^-$ and CD43 1B11$^+$ T cells after transplantation **(Figure 3A)**. We isolated CD62L^{lo} CD43 1B11$^-$ and CD43 1B11$^+$ CD8$^+$ T cells from CD45.1 hosts that were grafted with Balb/c skin using flow cytometric sorting. We adoptively transferred equal numbers of these cells into CD45.2 C57Bl/6 mice, and challenged them with a Balb/c skin graft the following day. We evaluated the number and phenotype of transferred populations on day 21 post-graft. We found that relative to CD43 1B11$^-$ T cells, greater numbers of CD43 1B11$^+$ T cells were recovered from secondary lymphoid tissue **(Figure 3B)**. While CD43 1B11$^+$ T cells remained CD43 1B11$^+$ after skin grafting, a fraction of CD43 1B11$^-$ T cells converted to CD43 1B11$^+$ T cells following the second skin graft challenge. Together, these data demonstrate that CD43 1B11$^+$ CD8$^+$ T cells have properties of a terminal effector population, as they are formed from CD43 1B11$^-$ precursors. However, they also appear to be persistent relative to CD43 1B11- CD8+ t cells.

CD43 1D4 mAb identifies a population of effector CD8$^+$ T in healthy human donors and kidney transplant candidates

In humans, high and low molecular weight forms of the CD43 receptor have been identified.[29] However, the use of CD43 as a marker of CD8$^+$ T cells has not been explored. The CD43 1D4 mAb clone identifies a larger isoform of CD43 on human T cells. We explored the expression of CD43 1D4 on CD8$^+$ T cells on PBMC from healthy donors. We found that a fraction of CD8$^+$ T cells stained for CD43 1D4 **(Figure 4A)**. We investigated whether the CD43 1D4$^+$ CD8$^+$ T cells corresponded with the canonical populations of naïve (CCR7$^+$CD45RA^{hi}) or antigen-experienced populations: central memory (T_{CM}, CCR7$^+$CD45RA^{lo}), effector memory

(T_{EM}, CCR7$^-$CD45RA^{lo}), or T effector memory RA$^+$ (T_{EMRA}, CCR7$^-$CD45RA$^+$) populations. While CD43 ID4$^-$ CD8$^+$ T cells were predominantly phenotypically naïve, CD43 1D4$^+$ CD8$^+$ T cells were found within all antigen-experience fractions **(Figure 4B).** Further exploration of the phenotype of these cells revealed that CD43 1D4$^+$ CD8$^+$ T cells had lower expression of CD27 and higher expression of CXCR3 and ICOS than CD43 1D4$^+$ CD8$^+$ T cells **(Figure 4C)**.

We next investigated whether CD43 1D4 was expressed on CD8$^+$ T cells from renal transplant candidates. Similar to healthy donors, a population of CD8$^+$ T cells expressed CD43 1D4 **(Figure 4D)**. We found that relative to CD43 1D4$^-$, CD43 1D4$^+$ CD8$^+$ T cells had similar expression of CD45RA and CCR7, demonstrating that this population did not correspond to a canonical T_{EM}, T_{CM}, or T_{EMRA} populations, as with healthy donors. However, CD43 1D4$^+$ CD8$^+$ T cells had higher expression of ICOS and CXCR3 **(Figure 4E).** Overall, these data demonstrate that CD43 1D4 identifies a population of antigen-experienced CD8$^+$ T cells in human healthy donors and renal transplant candidates.

CD43 1D4$^+$ CD8$^+$ T cells are efficient cytokine producers relative to CD43 1D4$^-$ CD8$^+$ T cells

We next tested the functional capacity of CD43 1D4$^+$ and CD43 1D4$^-$ CD8$^+$ T cells to produce cytokine **(Figure 5A)**. We stimulated PBMC from healthy donors with CD3ε mAb for 18-20 hours. We first evaluated the impact of stimulation on CD43 1D4 expression and found that there was a slight change in the CD43 1D4 expression among both CD45RA^{hi} and CD45RA^{lo} populations **(Figure 5B)**. This change seemed to be predominantly from CD43 1D4$^-$ to CD43 1D4$^+$ within the CD45RA^{hi} and CD45RA^{lo} compartments. As a population of CD45RA^{hi} cells remained CD43 1D4$^-$, we presumed the main change is occurring among the antigen-experienced T_{EMRA} population, and that naïve CD8$^+$ T cells are not able to upregulate CD43 1D4 expression in this short timeframe.

We evaluated the cytokine production among three populations, CD45RA^{hi} CD43 1D4^{-}, CD45RA^{hi} CD43 1D4^{+}, and CD45R^{Alo} CD43 1D4^{+} cells **(Figure 5C)**. We excluded analysis of the the CD45RA^{lo} CD43 1D4^{-} quadrant, as there were very few cells present with this phenotype for most donors. We found that the majority of TNF-α and IFN-γ was produced by the CD45RA^{lo} CD43^{+} population **(Figure 5D)**. When we evaluated cytokine production as a part-of-whole analysis, we found that both CD43 1D4^{+} fractions produced elevated levels of TNF-α and IFN-γ relative to CD43 1D4^{-} fraction **(Figure 5D)**. In total, these data demonstrate that CD43 1D4 is a marker of antigen-experienced CD8^{+} cells that are poised to produce cytokine.

CD8^{+} T cells that are *SPN*$^{+}$*GCNT1*$^{+}$ are present in the rejecting allografts of kidney transplant patients experiencing acute rejection

In order to investigate whether a population of CD43 1D4^{+} CD8^{+} T cells could be identified in the allografts of kidney transplant patients during acute rejection, we explored the single cell RNA-sequencing data generated by Shi et al **(Figure 6A)**.[11] Among 3 kidney transplant patients undergoing acute cellular rejection, we identified 8 clusters of CD8^{+} T cells **(Figure 6B)**. All clusters expressed the CD43 gene *SPN*. The because the glycosyltransferase GCNT1 is responsible for glycosylating the CD43 receptor, we reasoned that *SPN*$^{+}$*GCNT1*$^{+}$ clusters could be a surrogate for CD43 1D4^{+} CD8^{+} T cells observed using flow cytometry. We found that clusters 1, 2, 4, and 6 were *SPN*$^{+}$*GCNT1*$^{+}$ **(Figure 6C)**. The *SPN*$^{+}$*GCNT1*$^{+}$ clusters were higher for Granzyme B (*GZB*) and lower for CD62L (*SELL*), which is consistent with the CD43 1B11^{+} CD8^{+} T cell population in mice. The *SPN*$^{+}$*GCNT1*$^{+}$ clusters expressed high levels of granzymes and perforin (*GZMA, GZMH, GZMK, PRF1*). Relative to GCNT1^{-} clusters present in the allograft, they expressed elevated transcripts for IFN-γ (*IFNG*), the chemokine CXCR3, and the co-receptors PD-1 and ICOS, which are markers of recent antigen encounter. Overall, these results reveal that populations of CD8^{+} T cells that are *SPN*$^{+}$*GCNT1*$^{+}$ are present in rejecting

kidney allografts, and these clusters have features of highly potent effectors that have recently encountered antigen.

DISCUSSION

In this study, we built upon our previous work which showed that graft-specific L^d $QL9^+$ $CD8^+$ T cells express the activated form of the siaolomucin CD43, defined by the 1B11 mAb.[24] CD43 is a surface receptor that is involved in T cell signaling, adhesion, and trafficking. The function of CD43 receptor signaling on T cells has been explored in viral infection, autoimmunity, and sepsis.[25,32–34] However, the functional role of CD43 $1B11^+$ $CD8^+$ T cells in transplantation is not defined. Specifically, we wanted to evaluate three key outstanding questions: is CD43 1B11 is a marker of short-lived, highly proliferative $CD8^+$ T cells after transplantation? Is the CD43 1B11 pathway critical for graft rejection or only a population marker? Does an analogous $CD43^+$ effector $CD8^+$ T cell population exist in humans?

Although CD43 $1B11^+$ $CD8^+$ T cells peak in frequency during acute rejection,[24] the proliferative capacity and fate of these cells was not defined. We evaluated the proliferating populations of $CD8^+$ T cells during acute rejection and compared them with established activation markers. While several surface receptors were sensitive but not specific for Ki67 expression, including $CD44^{hi}$ and $CD62L^{lo}$, we found that CD43 1B11 and ICOS were specific markers for $Ki67^+$ $CD8^+$ T cells. Using adoptive transfer, we showed that most divided $CD8^+$ T cells post-graft were CD43 $1B11^+$ and $ICOS^+$. Together, these data demonstrate that, independent of either MHC tetramers or Ki67, the CD43 $1B11^+ICOS^+$ are reasonable surrogate markers for graft-specific proliferating $CD8^+$ T cells.

We also found that CD43 1B11 mAb agonism *in vivo* provides a costimulatory signal to $CD8^+$ T cells. CD43 1B11 mAb treatment was able to break costimulation-blockade induced tolerance and elicit skin graft rejection in the majority of mice after Balb/c skin grafting. In the presence of costimulation blockade, graft rejection after 1B11 mAb treatment was associated with an increased frequency of $CD62L^{lo}CD27^{lo}$ effector $CD8^+$ T cells. Together, these results demonstrate that CD43 1B11 is a marker of proliferative cells and that this signaling pathway is critical for alloimmunity. Further studies are needed to evaluate the mechanisms by which CD43

1B11$^+$ CD8$^+$ T cells are activated by allogeneic antigen in the presence of costimulation blockade.

We also investigated the fate of CD43 1B11$^-$ and CD43 1B11$^+$ CD8$^+$ T cell after acute rejection. Using an adoptive transfer approach, we showed that CD43 1B11$^+$ cells are more persistent 21 days after grafting, and that these cells maintain their CD43 1B11$^+$ status during this time. In contrast, about half of CD43 1B11$^-$ CD8$^+$ T cells differentiate into CD43 1B11$^+$, demonstrating that during the acute/primary immune response, CD43 1B11$^+$ CD8$^+$ T cells are continually formed from CD43 1B11$^-$ CD8$^+$ T cell population. Future studies are needed to elucidate the long-term fate of CD43 1B11$^+$ CD8$^+$ T cells in vivo. Prior work has shown that a population of virus-specific CD8$^+$ T cells is CD43 1B11$^+$,[35] and our prior work has shown that a minority of graft-specific CD8$^+$ T cells express CD43 1B11.[24] However, the function of memory CD43 1B11$^+$ CD8$^+$ T cells and the population dynamics of CD43 1B11$^+$ CD8$^+$ T cells that lead to memory formation have not been explored.

In humans, we investigated the expression of CD43 using the mAb clone 1D4, which binds to the larger core-2 O-glycosylated isoform of the CD43 receptor.[36] This antibody clone has been used to study CD4$^+$ T cells, but the expression on CD8$^+$ T cells was not previously reported. We found that a portion of CD8$^+$ T cells expression 1D4, and that the CD43 1D4$^+$ CD8$^+$ T cells had an antigen-experienced phenotype that did not correlate strongly with the central, effector, effector memory RA profile. We also found that CD43 1D4$^+$ CD8$^+$ T cells are potent cytokine producers, as nearly all of the TNF-α and IFN-γ was produced by CD43 1D4 CD8$^+$ T cells. Finally, we showed that a population of graft-infiltrating *SPN*$^+$*GCNT1*$^+$ CD8$^+$ T cells are present during acute rejection in kidney transplant patients. Together, these results provide evidence that CD43 1D4$^+$ CD8$^+$ T cells are a population of antigen-experienced effector CD8$^+$ T cells that participate in acute allograft rejection in humans.

Acute T cell mediated rejection remains a risk factor for early graft loss. Despite the use of T cell targeting therapies (T cell depletion, calcineurin inhibitors), acute allograft rejection

occurs in 10-20% of solid organ transplant patients.[2,37] Thus, new targets and approaches are needed to reduce allograft rejection and improve long-term graft survival. While this work establishes CD43 1B11^{+} CD8^{+} T cells as important populations in the process of acute rejection, future mechanistic and translational studies are needed to explore the potential approaches to therapeutically target them.

FIGURE LEGENDS

Figure 1. Proliferative CD8$^+$ T cells are defined by CD43$^+$ and ICOS$^+$ phenotype after transplantation. (A-B) C57Bl/6 mice were provided with Balb/c skin grafts and CD8$^+$ T cells were assessed on day 14 post-graft in the spleen and graft draining lymph nodes. (B) Representative flow and summary data depicting the frequency of Ki67$^+$ cells among CD8$^+$ T cells expressing the indicated marker. (C) 2x10^6 naïve CD45.1 or 1x10^6 Thy1.1 OT-I CD8$^+$ T cells labeled with CellTrace Violet were adoptively transferred into CD45.2 C57Bl/6 mice, who were provided with Balb/c or Act-mOVA skin grafts, respectively. Transferred cells were enriched using paramagnetic beads specific for APC, which stained Thy1.1 or L^d QL9 tetramers. (D) Among the adoptively transferred CD8$^+$ T cell populations, gates were drawn around the undivided (gray) and proliferated (orange) populations. (E) The frequency of CD43$^+$ICOS$^+$ cells was assessed in each adoptively transferred CD8$^+$ T cell population. Each data point depicts an individual mouse. Summary data depicts pooled results from 2-3 independent experiments (n=5-10 mice/group). Statistics performed by (C) 1-way ANOVA or (E) mixed-effects model (REML) with Tukey's multiple comparisons test or (E) unpaired Student's t-test. Error bars depict SEM. *p<0.05, **p<0.01, ***p<0.001, ****p<0.0001.

Figure 2. Treatment with CD43 1B11 mAb can break costimulation-blockade induced tolerance. (A) C57Bl/6 mice were provided with Balb/c skin grafts and treated with tolerance-inducing costimulation-blockade with CTLA-4 Ig and CD154 mAb (250 ug/dose, day 0, 2, 4, 6). Groups of mice were treated with IgG2a isotype control or CD43 1B11 mAb (200 ug/dose) on day 8, 11, and 14. (B) On day 14 post-graft, the phenotype of CD8$^+$ T cells was assessed in the blood of skin grafted mice. (C) The expression of Ki67 was assessed on populations of CD8$^+$ T cells in the blood from B. (D) Skin graft survival was assessed on mice treated as described in A. Each data point depicts an individual mouse. Summary data depicts pooled results from 2 independent

experiments (n=6-8 mice/group). Statistics performed by (B) Student's t-test (2-tailed), (C) (C) 1-way ANOVA or (E) mixed-effects model (REML) with Tukey's multiple comparisons test or (E) unpaired Student's t-test. Error bars depict SEM. **p<0.01, ***p<0.001, ****p<0.0001.

Figure 3. CD43 1B11$^+$ CD8$^+$ T cells are persistent after grafting relative to CD43 1B11$^-$ CD8$^+$ T cells. (A) Effector CD45.1 CD8$^+$ T cells (day 10-14 after Balb/c skin grafts) were flow cytometrically sorted into CD43 1B11$^+$ and CD43 1B11$^-$ populations and 1x10^5 were adoptively transferred into C57Bl/6 (CD45.2) hosts, who were provided with Balb/c skin grafts the following day. Transferred cells were assessed on day 14 post-graft. (B) Recovery of CD43 1B11$^+$ and CD43 1B11$^-$ CD8$^+$ T cells in the secondary lymphoid organs. (C) Frequency of CD43 1B11$^+$ CD8$^+$ T cells among adoptively transferred populations. Summary data depicts pooled results from 3 independent experiments (n=6-10 mice/group). Statistics performed by (B-C) unpaired Student's t-test (2-tailed). Error bars depict SEM. *p<0.05, ***p<0.001.

Figure 4. A population of human CD8$^+$ T cells are CD43 1D4$^+$ and have an antigen-experienced effector phenotype. (A) The frequency of healthy donor PBMC that express the CD43 mAb 1D4 clone. (B-C) Among CD43 1D4$^+$ and 1D4$^-$ CD8$^+$ T cells, the expression of CD45RA and CCR7 among healthy human donors. (C) Representative flow plots and summary data showing expression of CD27, CXCR3, and ICOS among CD43 1D4$^+$ and 1D4$^-$ CD8$^+$ T cell populations. (D) Frequency of CD43 1D4$^+$ CD8$^+$ T cells among kidney transplant candidates. (E) Expression of CD45RA, CCR7, ICOS, CXCR3, and CD27 among CD43 1D4$^+$ and CD43 1D4$^-$ CD8$^+$ T cells. Each data point depicts an individual human donor. Summary data depicts pooled results from (A-C) 3 independent experiments (n=12-13 individuals/group) or (D-E) 2 independent experiments (n=6 individuals/group). Statistics performed by (B) 2-way ANOVA with Sidak's multiple comparisons test and (D-E) paired Student's t-test (2-tailed), Error bars depict SEM. *p<0.05, **p<0.01, ***p<0.001, ****p<0.0001.

Figure 5. Human CD43 1D4$^+$ CD8$^+$ T cell populations are potent cytokine producers relative to CD43 1D4$^-$ CD8$^+$ T cells. (A) Healthy donor PBMC were stimulated for 20-24 h with CD3ε mAb (OKT3) and assessed for TNF-α and IFN-γ production. (B) Representative flow cytometry plots and summary data showing expression of CD43 1D4 expression among CD45RA^{hi} and CD45RA^{lo} populations of CD8$^+$ T cells. (C) Representative flow cytometry plots showing the production of TNF-α and IFN-γ after CD3ε mAb stimulation. (D) Summary data depicting the proportion of TNF-a (left) or IFN-g (right) produced by each CD45RA and CD43 1D4 quadrant population. Each data point depicts an individual human donor. Summary data depicts pooled results from 3 independent experiments (n=12-13 individuals/group). Statistics performed by (B) paired Student's t-test (2-tailed), (D) repeated measures 1-way ANOVA with Dunnett's multiple comparisons test. Error bars depict SEM. **p<0.01, ****p<0.0001.

Figure 6. A population of effector-like graft-infiltrating CD8$^+$ T cells from kidney transplant patients are *SPN$^+$GCNT1$^+$*. (A) Biopsies from kidney transplant patients with clinical signs of acute rejection were analyzed by single cell RNA-sequencing. (B) Hierarchical clustering and U-MAP analysis of CD8$^+$ T cells from kidney allograft biopsies. (C) Expression of SPN, GCNT1, GZMB, SELL among CD8+ T cell clusters. (D) Heatmap depicting expression genes for T cell of co-receptor and effector proteins.

METHODS

Animals. C57BL/6J, C57BL/6J Ly5.2-Cr (CD45.1), C57Bl/6-Tg(TcraTcrb)1100Mjb/J (OT-I), and C567BL/6-Tg(CAG-OVAL)916Jen/J (Act-mOVA) were obtained from The Jackson Laboratory (Bar Harbor, Maine) and used at 6-12 weeks of age. Balb/cJ, were obtained from The Jackson Laboratory and bred at Johns Hopkins University. All transplant experiments were conducted in age-matched hosts randomly assigned to experimental groups. This study was conducted in accordance with the recommendations in the Guide for the Care and Use of Laboratory Animals. The protocol was approved by the Animal Care and Use Committee at Johns Hopkins University. Animals were housed in specific pathogen-free animal facilities at Johns Hopkins University.

Skin grafting and in vivo treatments. Full-thickness tail and ear skins were transplanted onto the dorsal thorax of recipient mice and secured with adhesive bandages as previously described (Trambley et al., 1999). In some experiments, mice were treated with 250 ug/dose of CTLA-4 Ig (BioXCell) and anti-CD40L (MR1 clone, BioXCell) via i.p. injection as indicated. CD43 1B11 mAb (Biolegend) was provided at 200 μg/dose via i.p. injection.

MHC Tetramers and Graft-Specific CD8$^+$ T cell Enrichment. MHC tetramers with human β2-microglobulin specific for QL9 (H-2L^d QLSPFPFDL) were obtained from the NIH Tetramer Core facility as biotinylated monomers. Tetramer production was performed by adding Streptavidin-APC according to the core facility protocol. Tetramer enrichment was performed based on published protocols (Moon et al., 2009). Briefly, single cell suspensions of splenocytes or lymphocytes were incubated with MHC tetramer (PE or APC), followed by incubation with anti-APC paramagnetic microbeads (Miltenyi), and enrichment over an LS column (Miltenyi). The column flow through was collected as the unbound fraction containing bulk CD8$^+$ T cells and the

column bound fraction enriched for tetramer binding cells were stained for surface and intracellular antigens and analyzed by flow cytometry.

Skin grafting and in vivo treatments. Full-thickness tail and ear skins were transplanted onto the dorsal thorax of recipient mice and secured with adhesive bandages as previously described (Trambley et al., 1999). In some experiments, mice were treated with 250 ug/dose of CTLA-4 Ig (BioXCell) and anti-CD40L (MR1 clone, BioXCell) via i.p. injection as indicated. CD43 1B11 mAb (Biolegend) was provided at 200 μg/dose via i.p. injection.

Flow cytometric cell sorting and adoptive transfer. To obtain effector $CD8^+$ T cells, splenocytes and graft draining lymph nodes (inguinal, brachial, axial) from $CD45.1^+$ mice grafted with Balb/c skin grafts 10-14 days prior were collected and processed to single cell suspension. For proliferation analysis, $CD8^+$ T cells were isolated using $CD8^+$ T cell negative selection kit (Miltenyi), and stained with CellTrace Violet (Invitrogen) according to manufacturer's instructions. $2x10^6$ cells were transferred into naïve C57Bl/6 mice via tail vein. The following day, Balb/c skin grafts were provided. To isolate CD43 1B11 populations, CD8+ T cells were flow cytometrically sorted into $CD44^{hi}CD62L^{lo}CD8^+$ T cells that were CD43 $1B11^+$ and CD43 $1B11^-$. Sorting was performed using a MoFlo XDP instrument. $0.9\text{-}1.2x10^5$ purified cells were transferred via tail vein into C57BL/6J mice. Mice were grafted the following day with Balb/c skin.

Murine T cell enrichment and flow cytometry. Flow cytometry and magnetic bead enrichment were performed in 1X PBS (without Ca^{2+}/Mg^{2+}, pH 7.2), 0.25% BSA, 2 mM EDTA, and 0.09% azide. In some experiments, after blocking for 15 min with Fc block (Biolegend and 2% rat and mouse sera, $CD45.1^+$ or L^d $QL9^+$ $CD8^+$ T cells were enriched using magnetic beads specific for fluorophores and LS columns (Miltenyi) as described. MHC tetramers with human β2-

microglobulin specific for QL9 (H-2L^d QLSPFPFDL) were obtained from the NIH Tetramer Core facility as biotinylated monomers. Single cell suspensions were incubated in 96-well U-bottom plates with the following antibodies for 30-60 min at room temperature: CD4, CD8, CD11c, F4/80, CD19, CD27, CD28, CD43 1B11, CD62L, ICOS, CD44, and CD62L. Intracellular staining was performed using the Transcription Factor Staining Kit (eBiosciences) and Ki67 antibody. Dead cells were excluded with Live/Dead NIR Zombie (Biolegend) according to manufacturer's instructions. Samples were acquired on a Cytek Aurora (4L and 5L configuration).

Human peripheral blood cell analysis. Healthy donors and kidney transplant candidates were isolated following protocols approved by the Johns Hopkins Institutional Review Board. Healthy donor peripheral blood was collected in Vacutainer tubes containing sodium heparin (BD Biosciences) and processed according to manufacturer's instructions to isolate mononuclear cells. In some cases, PBMC were cryopreserved in 10% DMSO for later batched analysis. For cytokine production, 1.0×10^6 PBMC were plated in 96 well U-bottom plates in complete RPMI with L-glutamine (10% FBS, 10 mM HEPES, 10 μM β-mercaptoethanol) for 20 h at 37 C. T cells were stimulated with 0.5 μg/mL CD3ε mAb (OKT3; ThermoFisher) for 20 hrs at 37 C in the presence of 10 μg/mL GolgiStop (ThermoFisher). For flow cytometry, $0.5\text{-}1.0 \times 10^6$ PBMC were added in U-bottom plates. Supernatant from 1D4 hybridoma was incubated for 30 min, followed by anti-mouse IgG PE, and the remaining surface antibody. Intracellular staining was performed using the Transcription Factor Staining Kit (eBiosciences) with TNF-α and IFN-γ antibodies. Dead cells were excluded with Live/Dead NIR Zombie (Biolegend) according to manufacturer's instructions. Samples were acquired on a Cytek Aurora (4L and 5L) instrument.

Human scRNAseq kidney transplant biopsy analysis. Biopsies were collected from kidney transplant patients experiencing acute rejection as described. Gene count matrices for the

samples were generated by CellRanger count, and analyzed in R (4.3.0) using Seurat (4.3.0.1). Cells with excluded with fewer than 200, more than 2500 gene counts, or greater than 20% mitochondrial DNA. Analysis was filtered on mature $CD8^+$ T cells defined as cells expressing at least one chain of CD3, CD8A, and not expressing CD4. The samples were integrated using the top 2000 genes and 50 dimensions. Dimensionality reductions and clustering analysis were generated using the first 12 dimensions and a resolution of 0.5. Relevant figures were generated with ggplot2 (3.4.3) and pheatmap (1.0.12).

Quantification and Statistical Analysis

Statistical Analysis. All data points represent individual mice, and where individual data points are not depicted the value of n is provided in the corresponding figure legend. For analysis of absolute numbers and expression levels, paired or unpaired Student's t-tests (two-tailed) were performed between two groups; one-way or two-way ANOVA with multiple comparison tests were used to compare multiple groups. Log-rank (Mantel-cox) test was used to evaluate graft survival between groups. Error bars represent standard error measurements (SEM). Statistics were performed using GraphPad Prism 9 or 10. Significance was determined as *$p<0.05$, **$p<0.01$, ***$p<0.001$, ****$p<0.0001$.

ACKNOWLEDGEMENTS

We thank the Johns Hopkins Collaborative Outcomes Research in Endocrine Surgery (CORES) for human subject sample collection and storage. We thank members of the Johns Hopkins Department of Pathology Division of Immunology for helpful discussions. We appreciate Hao Zhang and the Bloomberg School of Public Health Flow Cytometry and Cell Sorting Core for excellent cell sorting, and the NIH Tetramer Core Facility for tetramer reagents and technical advice. This work was supported by R56 AI179856 (S.M.K.), American Society of Transplantation Research Network Career Transition Grant (S.M.K.), and KidneyCure Carl W. Gottschalk Research Scholar Grant (S.M.K.).

AUTHOR CONTRIBUTIONS

Conceptualization, S.M.K., G.S.C.; methodology, G.S.C., S.M.K., C.M.; formal analysis, S.M.K., G.S.C.; investigation, G.S.C., J.S.F., R.P.L., R.H.; writing, S.M.K.; visualization, S.M.K., G.S.C.; supervision, S.M.K.

DECLARATION OF INTEREST

The authors declare no competing interests.

REFERENCES

1. Hart, A. *et al.* OPTN/SRTR 2019 Annual Data Report: Kidney. *Am. J. Transplant.* **21**, (2021).
2. Colvin, M. *et al.* OPTN/SRTR 2019 Annual Data Report: Heart. *Am. J. Transplant.* **21**, (2021).
3. Callemeyn, J. *et al.* Allorecognition and the spectrum of kidney transplant rejection. *Kidney Int.* (2021) doi:10.1016/j.kint.2021.11.029.
4. Loupy, A., Hill, G. S. & Jordan, S. C. The impact of donor-specific anti-HLA antibodies on late kidney allograft failure. *Nat. Rev. Nephrol.* **8**, (2012).
5. Cherukuri, A. *et al.* Transitional B cell cytokines predict renal allograft outcomes. *Sci. Transl. Med.* **13**, (2021).
6. Cole, E. H., Johnston, O., Rose, C. L. & Gill, J. S. Impact of Acute Rejection and New-Onset Diabetes on Long-Term Transplant Graft and Patient Survival. *Clin. J. Am. Soc. Nephrol.* **3**, (2008).
7. Adams, A. B., Ford, M. L. & Larsen, C. P. Costimulation Blockade in Autoimmunity and Transplantation: The CD28 Pathway. *J. Immunol.* **197**, 2045–2050 (2016).
8. Krummey, S. M. *et al.* Low-Affinity Memory CD8+ T Cells Mediate Robust Heterologous Immunity. *J. Immunol.* **196**, 2838–2846 (2016).
9. Ford, M. L. & Larsen, C. P. Overcoming the memory barrier in tolerance induction: molecular mimicry and functional heterogeneity among pathogen-specific T-cell populations. *Curr. Opin. Organ Transplant.* **15**, 405–410 (2010).
10. Mathews, D. V. *et al.* CD122 signaling in CD8+ memory T cells drives costimulation-independent rejection. *J. Clin. Invest.* **128**, 4557–4572 (2018).
11. Shi, T. *et al.* Single-cell transcriptomic analysis of renal allograft rejection reveals insights into intragraft TCR clonality. *J. Clin. Invest.* **133**, (2023).
12. Ford, M. L. T Cell Cosignaling Molecules in Transplantation. *Immunity* **44**, (2016).

13. Chung, H. K., McDonald, B. & Kaech, S. M. The architectural design of CD8+ T cell responses in acute and chronic infection: Parallel structures with divergent fates. *J. Exp. Med.* **218**, (2021).

14. Jameson, S. C. & Masopust, D. Understanding Subset Diversity in T Cell Memory. *Immunity* **48**, 214–226 (2018).

15. Zehn, D., Lee, S. Y. & Bevan, M. J. Complete but curtailed T-cell response to very low-affinity antigen. *Nature* **458**, 211–214 (2009).

16. Nolz, J. C. Molecular mechanisms of CD8+ T cell trafficking and localization. *Cell. Mol. Life Sci.* **72**, 2461–2473 (2015).

17. Herndler-Brandstetter, D. *et al.* KLRG1+ Effector CD8+ T Cells Lose KLRG1, Differentiate into All Memory T Cell Lineages, and Convey Enhanced Protective Immunity. *Immunity* **48**, 716-729.e8 (2018).

18. Joshi, N. S. *et al.* Inflammation Directs Memory Precursor and Short-Lived Effector CD8+ T Cell Fates via the Graded Expression of T-bet Transcription Factor. *Immunity* **27**, (2007).

19. Kanev, K. & Zehn, D. Origin and fine-tuning of effector CD8 T cell subpopulations in chronic infection. *Curr. Opin. Virol.* **46**, 27–35 (2021).

20. Im, S. J. *et al.* Defining CD8+ T cells that provide the proliferative burst after PD-1 therapy. *Nature* **537**, 417–421 (2016).

21. Cohen, G. S. *et al.* Transplantation elicits a clonally diverse CD8+ T cell response that is comprised of potent CD43+ effectors. *Cell Rep.* **42**, 112993 (2023).

22. Park, J. K. *et al.* Enhancement of T-cell activation by the CD43 molecule whose expression is defective in Wiskott–Aldrich syndrome. *Nature* **350**, 706–709 (1991).

23. Cannon, J. L. *et al.* CD43 interaction with ezrin-radixin-moesin (ERM) proteins regulates T-cell trafficking and CD43 phosphorylation. *Mol. Biol. Cell* **22**, 954–963 (2011).

24. Sperling, A. I. *et al.* CD43 is a murine T cell costimulatory receptor that functions independently of CD28. *J. Exp. Med.* **182**, 139–146 (1995).

25. Mody, P. D. *et al.* Signaling through CD43 regulates CD4 T-cell trafficking. *Blood* **110**, 2974–2982 (2007).

26. Nolz, J. C. & Harty, J. T. Protective Capacity of Memory CD8+ T Cells Is Dictated by Antigen Exposure History and Nature of the Infection. *Immunity* **34**, (2011).

27. Nolz, J. C. & Harty, J. T. IL-15 regulates memory CD8+ T cell O-glycan synthesis and affects trafficking. *J. Clin. Invest.* **124**, 1013–1026 (2014).

28. Perkey, E. *et al.* GCNT1-Mediated O-Glycosylation of the Sialomucin CD43 Is a Sensitive Indicator of Notch Signaling in Activated T Cells. *J. Immunol. Baltim. Md 1950* **204**, 1674–1688 (2020).

29. Mukasa, R. *et al.* Core 2-containing O-glycans on CD43 are preferentially expressed in the memory subset of human CD4 T cells. *Int. Immunol.* **11**, 259–268 (1999).

Figure 1

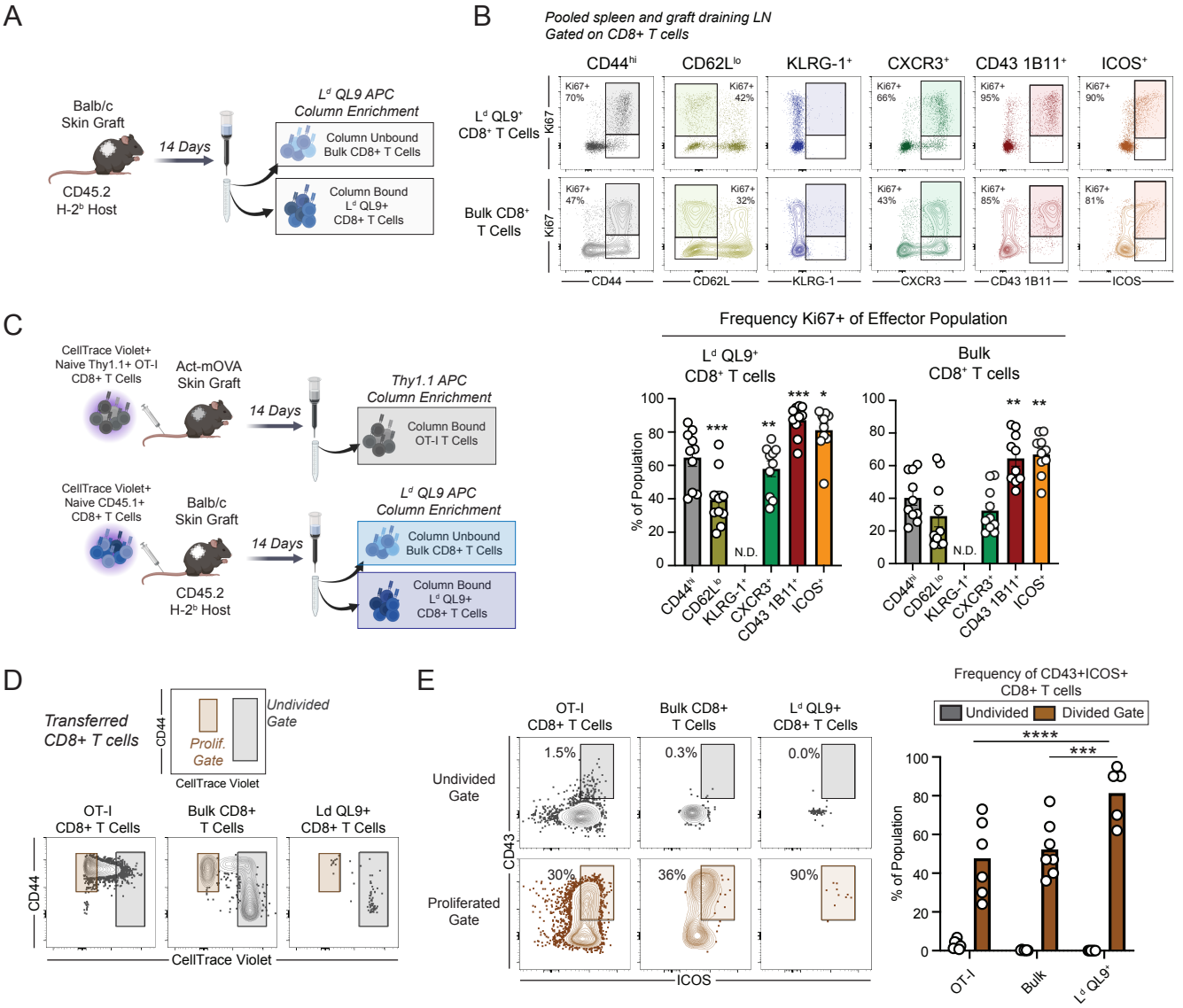
A
Balb/c
Skin Graft
CD45.2
H-2b Host
14 Days
Ld QL9 APC
Column Enrichment
Column Unbound
Bulk CD8+ T Cells
Column Bound
Ld QL9+
CD8+ T Cells
B
Pooled spleen and graft draining LN
Gated on CD8+ T cells
CD44hi
CD62Llo
KLRG-1+
CXCR3+
CD43 1B11+
ICOS+
Ld QL9+
CD8+ T Cells
Bulk CD8+
T Cells
Ki67
Ki67+ 70%
Ki67+ 42%
Ki67+ 66%
Ki67+ 95%
Ki67+ 90%
Ki67+ 47%
Ki67+ 32%
Ki67+ 43%
Ki67+ 85%
Ki67+ 81%
CD44
CD62L
KLRG-1
CXCR3
CD43 1B11
ICOS
C
CellTrace Violet+
Naive Thy1.1+ OT-I
CD8+ T Cells
Act-mOVA
Skin Graft
14 Days
Thy1.1 APC
Column Enrichment
Column Bound
OT-I T Cells
CellTrace Violet+
Naive CD45.1+
CD8+ T Cells
Balb/c
Skin Graft
CD45.2
H-2b Host
14 Days
Ld QL9 APC
Column Enrichment
Column Unbound
Bulk CD8+ T Cells
Column Bound
Ld QL9+
CD8+ T Cells
Frequency Ki67+ of Effector Population
Ld QL9+
CD8+ T cells
Bulk
CD8+ T cells
% of Population
N.D.
CD44hi
CD62Llo
KLRG-1+
CXCR3+
CD43 1B11+
ICOS+
D
Transferred
CD8+ T cells
CD44
Prolif.
Gate
Undivided
Gate
CellTrace Violet
OT-I
CD8+ T Cells
Bulk CD8+
T Cells
Ld QL9+
CD8+ T Cells
CD44
CellTrace Violet
E
OT-I
CD8+ T Cells
Bulk CD8+
T Cells
Ld QL9+
CD8+ T Cells
Undivided
Gate
Proliferated
Gate
1.5%
0.3%
0.0%
30%
36%
90%
CD43
ICOS
Frequency of CD43+ICOS+
CD8+ T cells
Undivided
Divided Gate
% of Population
OT-I
Bulk
Ld QL9+

Figure 2

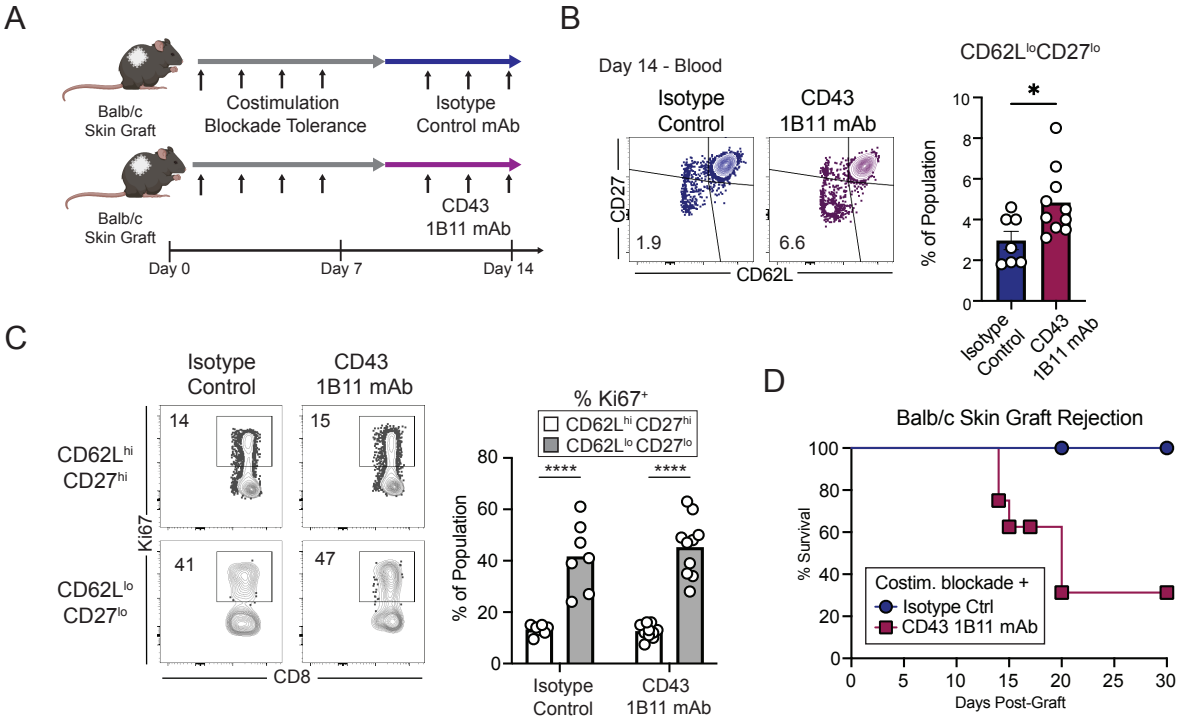
A
Balb/c
Skin Graft
Costimulation
Blockade Tolerance
Isotype
Control mAb
Balb/c
Skin Graft
CD43
1B11 mAb
Day 0
Day 7
Day 14
B
Day 14 - Blood
Isotype
Control
CD43
1B11 mAb
CD27
CD62L
1.9
6.6
CD62L^loCD27^lo
% of Population
Isotype
Control
CD43
1B11 mAb
C
Isotype
Control
CD43
1B11 mAb
CD62L^hi
CD27^hi
CD62L^lo
CD27^lo
Ki67
CD8
14
15
41
47
% Ki67+
CD62L^hi CD27^hi
CD62L^lo CD27^lo
% of Population
Isotype
Control
CD43
1B11 mAb
D
Balb/c Skin Graft Rejection
% Survival
Days Post-Graft
Costim. blockade +
Isotype Ctrl
CD43 1B11 mAb

Figure 3

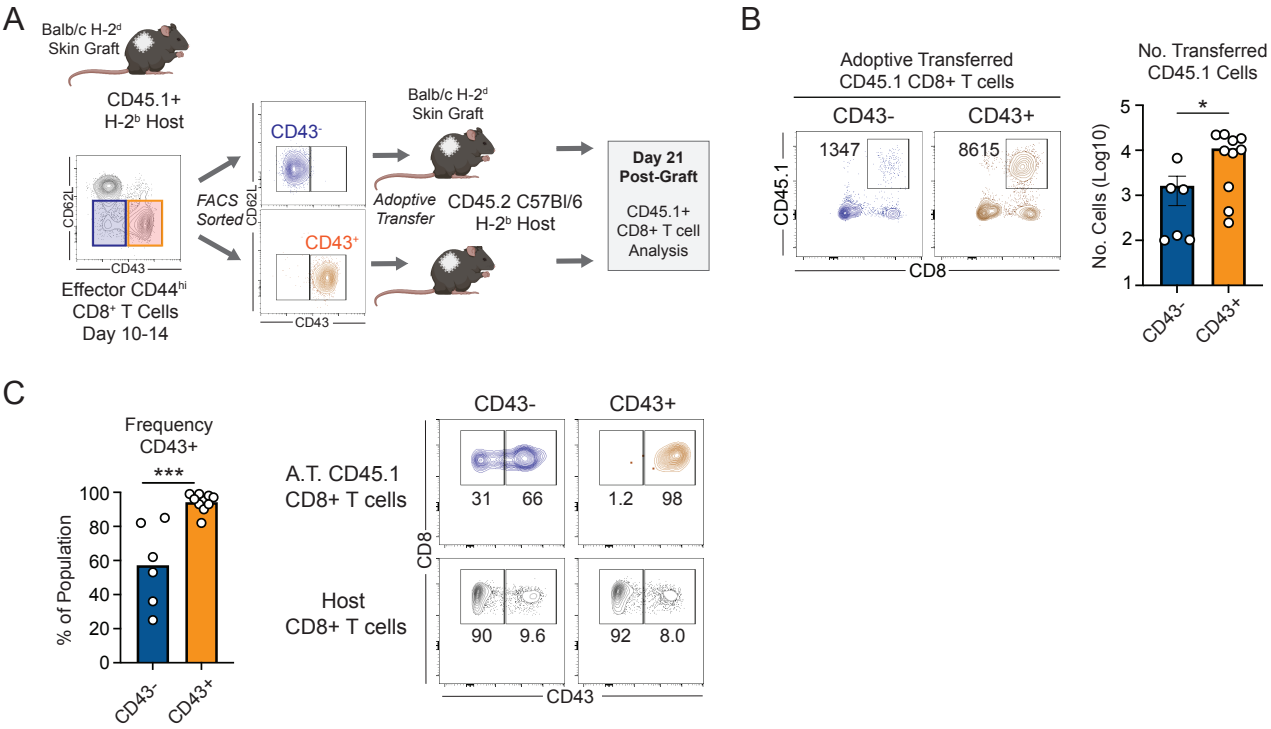
A
Balb/c H-2d Skin Graft
CD45.1+ H-2b Host
CD62L
CD43
Effector CD44hi CD8+ T Cells Day 10-14
FACS Sorted
CD43-
CD43+
Balb/c H-2d Skin Graft
Adoptive Transfer
CD45.2 C57Bl/6 H-2b Host
Day 21 Post-Graft
CD45.1+ CD8+ T cell Analysis
B
Adoptive Transferred CD45.1 CD8+ T cells
CD43-
CD43+
1347
8615
CD45.1
CD8
No. Transferred CD45.1 Cells
No. Cells (Log10)
*
CD43-
CD43+
C
Frequency CD43+
***
% of Population
CD43-
CD43+
A.T. CD45.1 CD8+ T cells
Host CD8+ T cells
31
66
1.2
98
90
9.6
92
8.0
CD8
CD43

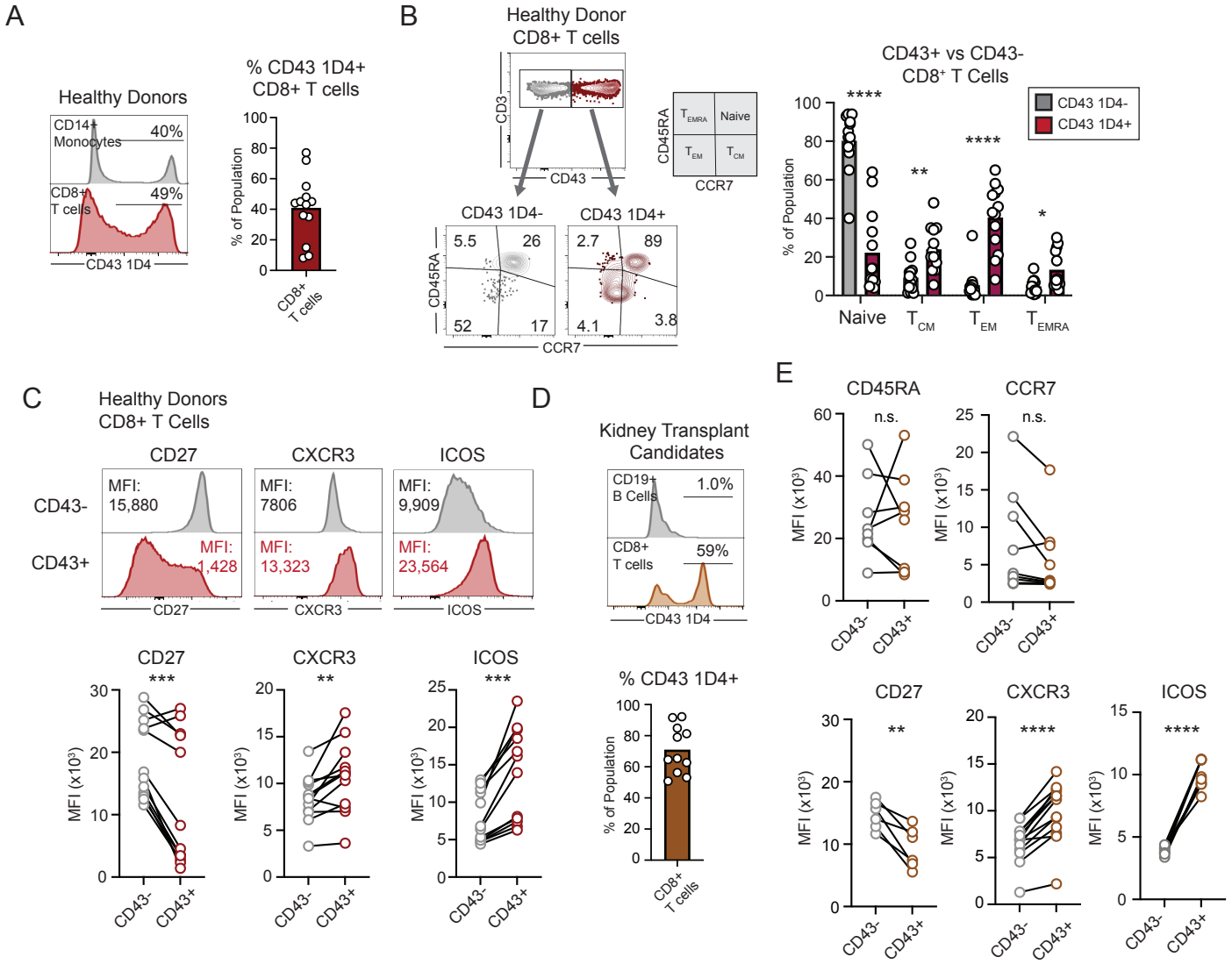
A
Healthy Donors
CD14+ Monocytes
40%
CD8+ T cells
49%
CD43 1D4
% CD43 1D4+ CD8+ T cells
% of Population
CD8+ T cells
B
Healthy Donor CD8+ T cells
CD3
CD43
CD45RA
CCR7
Naive
CD43 1D4-
CD43 1D4+
5.5
26
52
17
2.7
89
4.1
3.8
CD43+ vs CD43- CD8+ T Cells
CD43 1D4-
CD43 1D4+
Naive
C
Healthy Donors CD8+ T Cells
CD27
CXCR3
ICOS
CD43-
CD43+
MFI: 15,880
MFI: 1,428
MFI: 7806
MFI: 13,323
MFI: 9,909
MFI: 23,564
MFI (x10³)
D
Kidney Transplant Candidates
CD19+ B Cells
1.0%
CD8+ T cells
59%
% CD43 1D4+
E
CD45RA
CCR7
n.s.

Figure 5

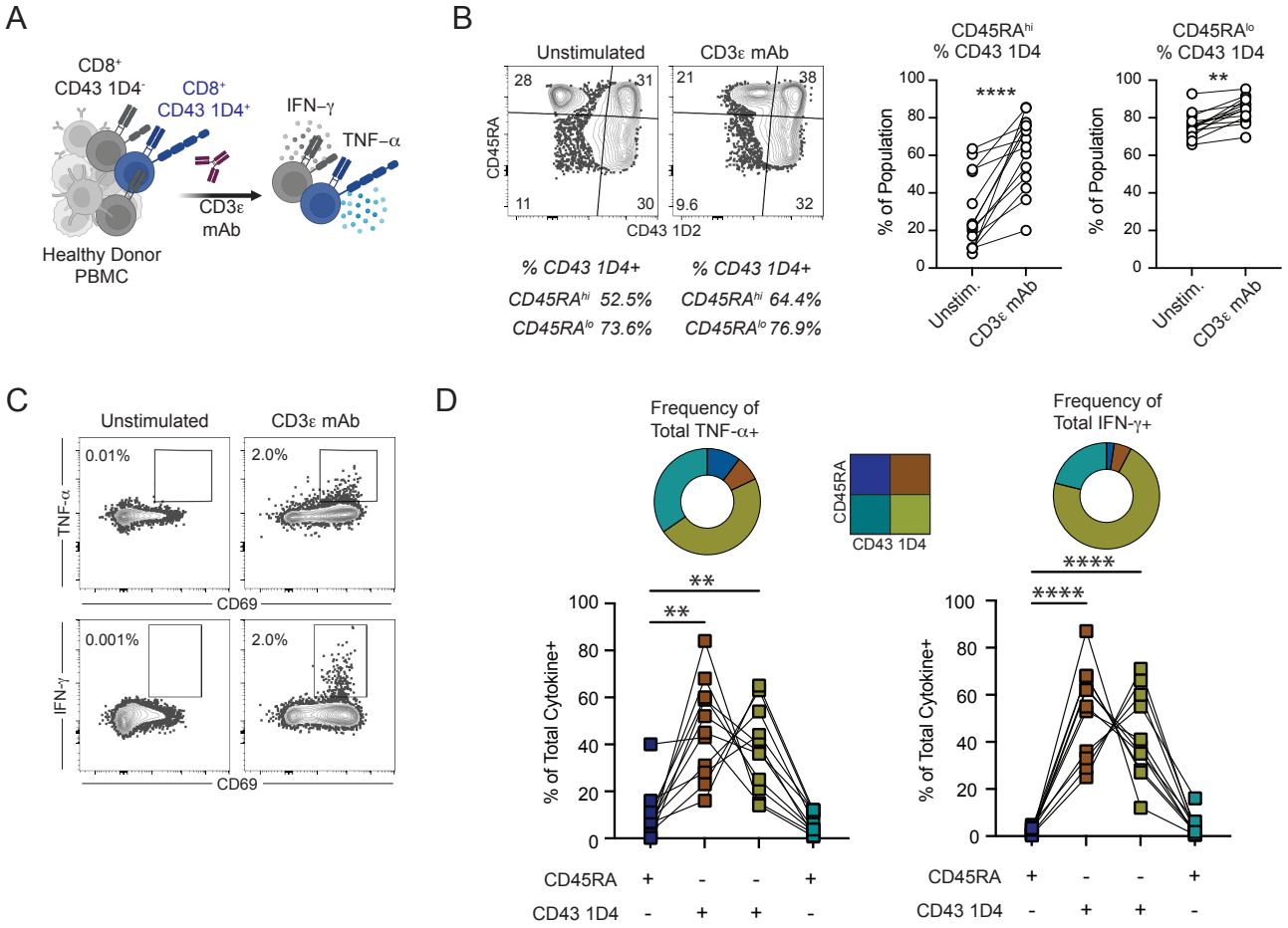
A
CD8+
CD43 1D4-
CD8+
CD43 1D4+
IFN–γ
TNF–α
CD3ε
mAb
Healthy Donor
PBMC
B
Unstimulated
CD3ε mAb
CD45RA
CD43 1D2
28
31
11
30
21
38
9.6
32
% CD43 1D4+
CD45RAhi 52.5%
CD45RAlo 73.6%
% CD43 1D4+
CD45RAhi 64.4%
CD45RAlo 76.9%
CD45RAhi
% CD43 1D4
CD45RAlo
% CD43 1D4
% of Population
****
**
Unstim.
CD3ε mAb
C
Unstimulated
CD3ε mAb
TNF-α
IFN-γ
CD69
0.01%
2.0%
0.001%
2.0%
D
Frequency of
Total TNF-α+
Frequency of
Total IFN-γ+
CD45RA
CD43 1D4
% of Total Cytokine+
**
****
CD45RA + - - +
CD43 1D4 - + + -

Figure 6

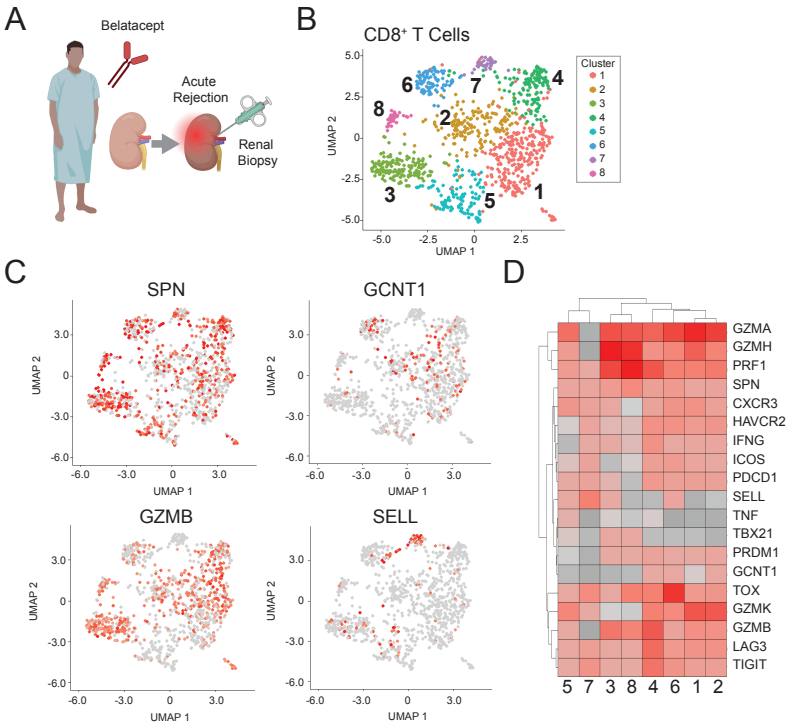
A
Belatacept
Acute Rejection
Renal Biopsy
B
CD8⁺ T Cells
Cluster
1
2
3
4
5
6
7
8
UMAP 1
UMAP 2
C
SPN
GCNT1
GZMB
SELL
D
GZMA
GZMH
PRF1
SPN
CXCR3
HAVCR2
IFNG
ICOS
PDCD1
SELL
TNF
TBX21
PRDM1
GCNT1
TOX
GZMK
GZMB
LAG3
TIGIT
5 7 3 8 4 6 1 2